SIAM J. IMAGING SCIENCES
Vol. 8, No. 1, pp. 1–18

Modelling the Effect of Focusing Detectors in Photoacoustic Sectional Imaging*

P. Elbau† and O. Scherzer‡

Abstract. To effectively use photoacoustic tomography to obtain cross-sectional images, a combination of a focused laser illumination and focusing acoustic detectors is used. In this work, we discuss how to incorporate cylindrically shaped focusing detectors in the mathematical modelling of photoacoustics and derive approximative reconstruction formulas. Moreover, we show how such focusing detectors combined with a focused illumination can yield a quantitative reconstruction of the material properties (the transport coefficient and the product of the Grüneisen parameter and the absorption coefficient) of a weakly scattering medium.

Key words. quantitative photoacoustic imaging, sectional imaging, reconstruction formulas, focusing detectors, single scattering

AMS subject classifications. 35L05, 35R30, 44A12, 45Q05

DOI. 10.1137/120882962

1. Introduction.

In photoacoustic imaging (see, for example, [38, 19, 15, 34] for some mathematical and physical review papers), the interior of a small object is analyzed by illuminating it with a short laser pulse and observing the acoustic wave which is thereby induced via the photoacoustic effect.

The measurement of this pressure wave allows us (under the assumption that the acoustic wave travels with constant velocity and is free from any attenuation effects) to recover internal measurements in the form of the initially generated pressure distribution caused by the absorption of the laser light; see, for instance, [12, 37] for some common reconstruction formulas for the initial pressure.

This initial pressure depends on the thermodynamic (via the Grüneisen parameter) and the optical (via the absorption coefficient of the laser light) properties of the medium, and on the total light fluence of the laser pulse at each position in the medium. To obtain a quantitative reconstruction of the material properties, we therefore additionally need to model the propagation of the laser light inside the medium.

A standard model for the light propagation is the radiative transfer equation. In biological tissues, the simpler diffusion approximation of the radiative transfer equation, which is valid for strongly scattering media, can often also be used.

For both of these light propagation models, there exist results about the reconstruction

*Received by the editors June 29, 2012; accepted for publication (in revised form) July 24, 2014; published electronically January 6, 2015. This work has been supported by the Austrian Science Fund (FWF) within the national research network "Photoacoustic Imaging in Biology and Medicine" (S10505-N20) and within the project "Interdisciplinary Coupled Physic Imaging" (P26687).

http://www.siam.org/journals/siims/8-1/88296.html

†Computational Science Center, University of Vienna, A-1090 Vienna, Austria (peter.elbau@univie.ac.at).

‡Johann Radon Institute for Computational and Applied Mathematics (RICAM), A-4040 Linz, Austria, and Computational Science Center, University of Vienna, A-1090 Vienna, Austria (otmar.scherzer@univie.ac.at).

of the material properties (the Grüneisen parameter and the absorption and scattering coefficient) from the reconstructed initial pressure; see [3, 23] for the radiative transfer equation and [2] for the diffusion approximation.

In practice, it is sometimes not very convenient to perform three-dimensional photoacoustic measurements, that is, illuminating the whole sample and then measuring the resulting acoustic wave on a two-dimensional surface around the object as a function of time, since doing these measurements can take a lot of time. Moreover, the object may possess some obstacles preventing the illumination of some regions or severely disturbing the propagation of the acoustic wave so that a complete reconstruction can be prone to errors.

We want to circumvent these problems by focusing the illumination onto a single slice of the object and then reconstructing the physical parameters there from a measurement of the acoustic wave along a curve encircling this slice, thus reducing the number of measurements by one dimension.

If the scattering in the object is negligible, the focusing of the light illumination will ensure that the measurements depend only on the material properties of the object in this slice, so that an exact reconstruction becomes possible; see [9]. However, typically the scattering in the medium cannot be neglected, so that signals from regions outside this cross section also will contribute to the measurements.

To suppress this effect, focusing acoustic detectors, which should mainly register acoustic waves originating from the desired section, are used. In the simplest case, these are cylindrically shaped integrating detectors whose axes lie in the plane of the section. Then, at least close to the axis of the detector, mainly the signals from the section should be recorded.

This photoacoustic sectional imaging method is already used in practice, and we refer to [21, 31, 32] and [13, 25, 28, 27] for some experimental setups and measurement data.

Furthermore, we would like to mention that, due to the fact that this method allows us to gather data localized to an arbitrary slice of the object, we may gain additional information (compared to the usual three-dimensional photoacoustic measurement) by performing a sectional measurement for every possible choice of slice through the object. This additional information could be used, for instance, to reconstruct an unknown, variable speed of sound in the model; see [14].

The aim of this paper is to study the reconstruction of the initial pressure and the physical parameters of the sample for a photoacoustic sectional imaging setup with focusing detectors. We derive in section 2 the forward model for the measurements obtained from a cylindrically shaped focusing detector and show how an approximate reconstruction of the initial pressure distribution in the vicinity of the axis of the cylindrical detector is possible.

In section 3, we remark that if the illumination remains (in spite of the scattering effects) focused onto a small neighborhood of the illuminated slice, then this approximate reconstruction may be extended to the whole section.

Finally, in section 4, we combine the reconstruction formula with a single scattering light propagation model to obtain a reconstruction formula for the physical material properties of the sample in the vicinity of the axis of the detector.

2. Photoacoustic imaging with focusing detectors. We consider a classical photoacoustic measurement. That is, we illuminate an object with a short laser pulse which induces via the photoacoustic effect an initial pressure[1] density $p : \mathbb{R}^3 \to \mathbb{R}$ in the object.

This initial pressure then initiates an acoustic wave $P : \mathbb{R} \times \mathbb{R}^3 \to \mathbb{R}$ propagating through the object. We want to use the simple model of a homogeneous, elastic medium with constant speed of sound c_s for the object. Then, linear elasticity theory leads us to the linear wave equation

$$\begin{aligned} \partial_{tt}P(t,x) &= c_\mathrm{s}^2\Delta_x P(t,x), && t>0,\ x\in\mathbb{R}^3, \\ \partial_t P(0,x) &= 0, && x\in\mathbb{R}^3, \\ P(0,x) &= p(x), && x\in\mathbb{R}^3, \end{aligned} \tag{2.1}$$

for the pressure density $P(t,x)$ at a point $x \in \mathbb{R}^3$ at time $t > 0$; see, for example, [15].

For standard photoacoustic measurements, this pressure wave is then recorded on the boundary ∂X of some domain X containing the object, yielding the data $P(t,x)$ for all $t > 0$ and all $x \in \partial X$. There are a lot of results about the reconstruction of the initial pressure p from these data: Explicit reconstruction formulas were obtained by Fourier methods [36, 39, 40] leading to the so-called universal back-projection formula [37, 24], which holds at least for the case where X is a half-plane, a cylinder, or an ellipsoid. Other approaches [12, 11, 17, 18, 16], reducing the problem to the inversion of the spherical means operator, also led to explicit reconstruction formulas for simple geometries X. In addition, from the more general setting of integral geometry used in [26], reconstruction formulas for the photoacoustic problem are also available.

However, we do not want to consider a complete reconstruction of p, but only determine the initial pressure p in the plane $E = \{x \in \mathbb{R}^3 \mid x_3 = 0\}$. To this end, we do not intend to use measurements on a surface ∂X, but only measurements on a circle in the plane E around the object. To diminish the effect from signals originating from points outside the plane E, we use at every position on the circle not a point detector but a cylindrically shaped, integrating detector; see, for example, [31, 28].

We model this detector explicitly as a cylindrical surface with axis in the illumination plane E going through the origin along the direction $(\theta, 0) \in \mathbb{R}^2 \times \mathbb{R}$, with radius R and with opening angle 2α. Thus, this yields the measurements

$$m_\theta(t) = \int_{-\infty}^{\infty}\int_{-\alpha}^{\alpha} P(t, x_1\theta + R\cos\varphi\,\theta^\perp, R\sin\varphi)\,\mathrm{d}\varphi\,\mathrm{d}x_1, \quad t>0, \tag{2.2}$$

where $\theta^\perp \in S^1$ denotes a vector orthogonal to θ, and where the measurements are done for every orientation $\theta \in S^1$ of the detector.

Lemma 2.1. *Let $P \in C^2([0,\infty) \times \mathbb{R}^3)$ be a solution of the initial value problem (2.1) for some function $p \in C_\mathrm{c}^3(\mathbb{R}^3)$, and let m be given by (2.2) for some $\alpha > 0$ and $R > 0$.*

Then, for every $\theta \in S^1$, the averaged initial pressure

$$\bar{p}_\theta(x_2,x_3) = \int_{-\infty}^{\infty} p(x_1\theta + x_2\theta^\perp, x_3)\,\mathrm{d}x_1, \quad x_2,x_3\in\mathbb{R}, \tag{2.3}$$

[1] More precisely, we should refer to it as a pressure difference to the equilibrium pressure in the object.

along the lines parallel to the axis of the detector fulfills the equation

$$M_\theta(\rho) = \int_{-\alpha}^{\alpha}\int_0^{2\pi} \bar p_\theta\left(R\begin{pmatrix}\cos\varphi\\ \sin\varphi\end{pmatrix} + \rho\begin{pmatrix}\cos\phi\\ \sin\phi\end{pmatrix}\right) \mathrm{d}\phi\,\mathrm{d}\varphi, \quad \rho > 0, \tag{2.4}$$

where the function $M_\theta : (0,\infty) \to \mathbb{R}$ *is explicitly given by*

$$M_\theta(\rho) = 4\int_0^{\frac{\rho}{c_\mathrm{s}}} \frac{m_\theta(t)}{\sqrt{\rho^2 - c_\mathrm{s}^2 t^2}} c_\mathrm{s}\,\mathrm{d}t. \tag{2.5}$$

Proof. Solving the wave equation (2.1) with Kirchhoff's formula (see, for instance, [10]), we obtain

$$P(t,x) = \partial_t \frac{t}{4\pi}\int_0^{\pi}\int_0^{2\pi} p\left(x + c_\mathrm{s} t\begin{pmatrix}\cos\vartheta\\ \sin\vartheta\cos\phi\\ \sin\vartheta\sin\phi\end{pmatrix}_\theta\right)\sin\vartheta\,\mathrm{d}\phi\,\mathrm{d}\vartheta,$$

where we used spherical coordinates with respect to the orthonormal basis $(\theta, 0)$, $(\theta^\perp, 0)$, $(0,0,1) \in \mathbb{R}^3$ to parametrize the integral over the sphere $\partial B_{c_\mathrm{s}t}(x)$. Here, the vector notation with the index θ shall be understood as the vector with respect to this orthonormal basis.

Plugging this expression for P into the definition (2.2) of the measurements m, we find that

$$m_\theta(t) = \partial_t \frac{t}{4\pi}\int_{-\infty}^{\infty}\int_{-\alpha}^{\alpha}\int_0^{\pi}\int_0^{2\pi} p\left(\begin{pmatrix}x_1 + c_\mathrm{s} t\cos\vartheta\\ R\cos\varphi + c_\mathrm{s} t\sin\vartheta\cos\phi\\ R\sin\varphi + c_\mathrm{s} t\sin\vartheta\sin\phi\end{pmatrix}_\theta\right)\sin\vartheta\,\mathrm{d}\phi\,\mathrm{d}\vartheta\,\mathrm{d}\varphi\,\mathrm{d}x_1.$$

Using the averaged pressure (2.3) and remarking that (after performing the integration over the variable x_1) the variable ϑ only enters via $\sin\vartheta$ so that the integrand is invariant under the reflection $\vartheta \mapsto \pi - \vartheta$, we find that

$$m_\theta(t) = \partial_t \frac{t}{2\pi}\int_{-\alpha}^{\alpha}\int_0^{\frac{\pi}{2}}\int_0^{2\pi} \bar p\left(R\begin{pmatrix}\cos\varphi\\ \sin\varphi\end{pmatrix} + c_\mathrm{s} t\sin\vartheta\begin{pmatrix}\cos\phi\\ \sin\phi\end{pmatrix}\right)\sin\vartheta\,\mathrm{d}\phi\,\mathrm{d}\vartheta\,\mathrm{d}\varphi.$$

Then, with the coordinate transform $\rho = c_\mathrm{s} t\sin\vartheta$, we obtain

$$m_\theta(t) = \partial_t \frac{1}{2\pi c_\mathrm{s}}\int_0^{c_\mathrm{s}t} \frac{\rho}{\sqrt{c_\mathrm{s}^2 t^2 - \rho^2}}\int_{-\alpha}^{\alpha}\int_0^{2\pi} \bar p_\theta\left(R\begin{pmatrix}\cos\varphi\\ \sin\varphi\end{pmatrix} + \rho\begin{pmatrix}\cos\phi\\ \sin\phi\end{pmatrix}\right)\mathrm{d}\phi\,\mathrm{d}\varphi\,\mathrm{d}\rho.$$

Now, this has the form of the solution of the generalized Abel integral equation[2]

$$4\int_0^{\frac{\rho}{c_\mathrm{s}}} \frac{m_\theta(t)}{\sqrt{\rho^2 - c_\mathrm{s}^2 t^2}} c_\mathrm{s}\,\mathrm{d}t = \int_{-\alpha}^{\alpha}\int_0^{2\pi} \bar p_\theta\left(R\begin{pmatrix}\cos\varphi\\ \sin\varphi\end{pmatrix} + \rho\begin{pmatrix}\cos\phi\\ \sin\phi\end{pmatrix}\right)\mathrm{d}\phi\,\mathrm{d}\varphi$$

for the function m_θ, which is just (2.4). ■

[2] We recall (see [29, Chapter 1.1.41] or [30, Chapter 8.10]) that the generalized Abel integral equation $f(s) = \int_0^s \frac{g(t)}{\sqrt{s^2-t^2}}\,\mathrm{d}t$, $s > 0$, has for given function $f \in C^1([0,\infty))$ the solution $g(t) = \frac{1}{\pi}\frac{\mathrm{d}}{\mathrm{d}t}\int_0^t \frac{2uf(u)}{\sqrt{t^2-u^2}}\,\mathrm{d}u$, $t > 0$.

We remark that the averaged pressure, defined in (2.3), can be written as

$$\bar{p}_\theta(x_2, x_3) = \mathcal{R}[p(\cdot, x_3)](x_2, \theta), \tag{2.6}$$

where $\mathcal{R}$ denotes the Radon transform.[3] Therefore, if we can recover the function $\bar{p}$, an inverse Radon transform gives us the initial pressure p.

To get a better intuition into which values of the initial pressure influence the measurements, we rewrite the integral in formula (2.4).

Lemma 2.2. *Let $R > 0$, $\alpha > 0$. Then we have for every function $\bar{p}_\theta \in C(\mathbb{R}^2)$ and every $\rho > 0$ with $\rho \neq R$ the identity*

$$\begin{aligned}\int_{-\alpha}^{\alpha}\int_0^{2\pi} \bar{p}_\theta\left(R\begin{pmatrix}\cos\varphi\\ \sin\varphi\end{pmatrix} + \rho\begin{pmatrix}\cos\phi\\ \sin\phi\end{pmatrix}\right) \mathrm{d}\phi\,\mathrm{d}\varphi \\ = \left(\int_{E_{1,\rho}} + 2\int_{E_{2,\rho}}\right) \frac{2\bar{p}_\theta(\xi)}{\sqrt{|\xi|^2 - (R-\rho)^2}\sqrt{(R+\rho)^2 - |\xi|^2}}\,\mathrm{d}\xi,\end{aligned} \tag{2.7}$$

where the domains $E_{i,\rho}$, $i = 1, 2$, are defined as the interior of the sets of all points $\xi \in \mathbb{R}^2$ such that the circle around ξ with radius ρ has exactly i intersection points with the arc

$$A_{R,\alpha} = \{(R\cos\varphi, R\sin\varphi) | \varphi \in (-\alpha, \alpha)\};$$

see Figure 1.

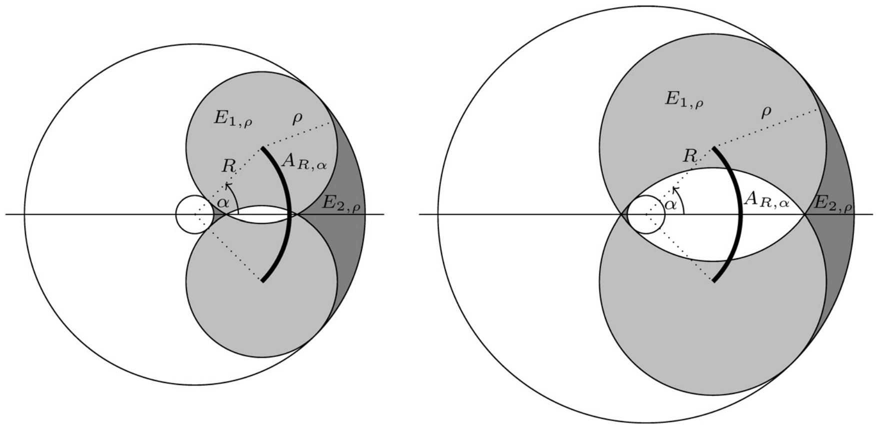

Figure 1. *The domains of integration $E_{1,\rho}$ and $E_{2,\rho}$ for a specified radius $\rho < R$ and $\rho > R$, respectively.*

Proof. We introduce the function

$$\psi(\varphi, \phi) = R\begin{pmatrix}\cos\varphi\\ \sin\varphi\end{pmatrix} + \rho\begin{pmatrix}\cos\phi\\ \sin\phi\end{pmatrix}.$$

Its Jacobi determinant is given by

$$|\det \mathrm{d}\psi(\varphi, \phi)| = R\rho|\sin(\phi - \varphi)|,$$

[3]We define the Radon transform $\mathcal{R}f : \mathbb{R} \times S^1 \to \mathbb{R}$ of an integrable function $f : \mathbb{R}^2 \to \mathbb{R}$ by $\mathcal{R}f(r, \theta) = \int_{-\infty}^{\infty} f(\lambda\theta + r\theta^\perp)\,\mathrm{d}\lambda$, $r \in \mathbb{R}$, $\theta \in S^1$; see, for instance, [30, Chapter 8].

so that ψ is a local diffeomorphism around all points (ϕ,φ) with $\phi-\varphi\notin\pi\mathbb{Z}$. Moreover, using that

$$|\psi(\varphi,\phi)|^2 = R^2+\rho^2+2R\rho\cos(\phi-\varphi),$$

we can write the Jacobi determinant in the form

$$\begin{aligned}|\det \mathrm{d}\psi| &= \sqrt{R^2\rho^2-\tfrac{1}{4}(|\psi|^2-R^2-\rho^2)^2}\\ &= \frac{1}{2}\sqrt{|\psi|^2-(R-\rho)^2}\sqrt{(R+\rho)^2-|\psi|^2}.\end{aligned}$$

To determine the inverse of ψ, we remark that if $\xi=\psi(\phi,\varphi)$, then the angles ϕ and φ can be found by taking an intersection point $\eta\in\partial B_\rho(\xi)\cap A_{R,\alpha}$. Then, the polar angle of η gives the angle φ, and the polar angle of $\xi-\eta$ is ϕ. This shows that for every point $\xi\in E_{1,\rho}$, there exists a unique inverse $\psi^{-1}(\xi)$, and for a point $\xi\in E_{2,\rho}$, the inverse $\psi^{-1}(\xi)$ consists of two points. The points outside of $\overline{E_{1,\rho}\cup E_{2,\rho}}$ are not in the range of ψ.

Thus, with the substitution $\xi=\psi(\varphi,\phi)$ the integral on the left-hand side of (2.7) is transformed to the integrals on the right-hand side.

To obtain the geometry of the sets $E_{i,\rho}$, drawn in Figure 1, we remark that the number of intersection points of $\partial B_\rho(\xi)\cap A_{R,\alpha}$ is a locally constant function of ξ unless the circle $\partial B_\rho(\xi)$ touches $A_{R,\alpha}$, which can happen only for $\xi\in\partial D$, where $D=B_{R+\rho}(0)\setminus B_{|R-\rho|}(0)$, or if one of the intersection points is at one of the endpoints of the arc, which happens if $\xi\in\partial B_+\cup\partial B_-$, where $B_\pm=B_\rho(R\cos\alpha,\pm R\sin\alpha)$ denote the balls with radius ρ around the points at the boundary of the detector.

These lines divide the annulus D (which is the image of ψ for $\alpha=\pi$) into four (if B_+ and B_- do not intersect) or six domains. Considering a particular point inside each of these regions, it is not hard to see that $E_{1,\rho}$ is always given by the symmetric difference

$$E_{1,\rho}=B_+\Delta B_-, \tag{2.8}$$

and $E_{2,\rho}$ is given by

$$E_{2,\rho}=C_+\setminus(B_+\cup B_-)\cup(C_-\cap B_+\cap B_-), \tag{2.9}$$

where the second term is empty for $\rho<R$.

Here, we used the notation

$$C_\pm=\{(\pm r\cos\beta,r\sin\beta)\in D\mid\beta\in(-\alpha,\alpha),\ r\in(|R-\rho|,R+\rho)\}. \qquad\blacksquare$$

In general, especially the integration over the domain $E_{1,\rho}$ shows that by no means are only signals from the plane E contributing to our measurements. However, if we consider the asymptotic case where the radius R of the detector is large compared to the diameter of the support of the initial pressure p and take $\alpha=\frac{\pi}{2}$ (meaning that we consider a half-cylinder as detector), some of these contributions can be cancelled out by taking the difference of the data $M_\theta(\rho)$ and $M_{-\theta}(\rho)$.

Proposition 2.3. *Let $P\in C^2([0,\infty)\times\mathbb{R}^3)$ be a solution of the initial value problem* (2.1) *for some function $p\in C_c^3(\mathbb{R}^3)$, and let m be given by* (2.2) *with $\alpha=\frac{\pi}{2}$.*

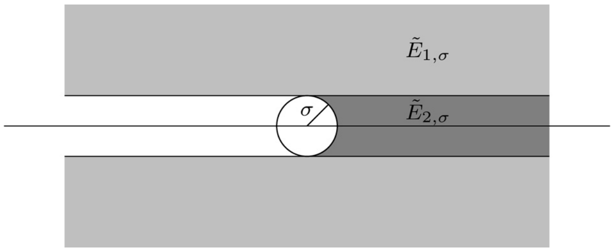

Figure 2. *The domains of integration in the case $\alpha = \frac{\pi}{2}$ and in the limit $R \to \infty$.*

Then, we have for every $\theta \in S^1$ and $\sigma > 0$ that the averaged pressure $\bar{p}_\theta$, given by (2.3), fulfills the integral equation

$$\tilde{M}_\theta(\sigma) = \int_{\tilde{E}_{2,\sigma}} \frac{\bar{p}_\theta(\xi) - \bar{p}_\theta(-\xi)}{\sqrt{|\xi|^2 - \sigma^2}} \,\mathrm{d}\xi, \tag{2.10}$$

where the function $\tilde{M}_\theta$ can be explicitly determined from the measurements m_θ via

$$\tilde{M}_\theta(\sigma) = \lim_{R\to\infty} \frac{R}{2}(M_\theta(R-\sigma) - M_{-\theta}(R-\sigma)), \tag{2.11}$$

with M_θ defined as in (2.5), and

$$\tilde{E}_{2,\sigma} = \{\xi \in \mathbb{R}^2 \mid \xi_1 > 0,\ |\xi| > \sigma,\ |\xi_2| < \sigma\}. \tag{2.12}$$

Proof. Combining Lemmas 2.1 and 2.2, we have that

$$M_\theta(\rho) = \left(\int_{E_{1,\rho}} +2\int_{E_{2,\rho}}\right) \frac{2\bar{p}_\theta(\xi)}{\sqrt{|\xi|^2 - (R-\rho)^2}\sqrt{(R+\rho)^2 - |\xi|^2}} \,\mathrm{d}\xi,$$

where the domains $E_{1,\rho}$ and $E_{2,\rho}$ are defined as in Lemma 2.2.

Now, in the case $\alpha = \frac{\pi}{2}$, we see from Figure 1 or analytically from (2.8) that

$$E_{1,\rho} = B_\rho(0,R)\Delta B_\rho(0,-R).$$

Therefore, in the limit $R \to \infty$, the integration of a function with compact support over the domain $E_{1,R-\sigma}$ converges for $R \to \infty$ to the integration over the domain

$$\tilde{E}_{1,\sigma} = \mathbb{R}^2 \setminus \{\xi \in \mathbb{R}^2 \mid |\xi_2| > \sigma\}, \quad \sigma > 0;$$

see Figure 2.

Similarly, we find from Figure 1 or analytically from (2.9) that

$$E_{2,\rho} = C_+ \setminus (B_\rho(0,R) \cup B_\rho(0,-R))$$

for $\rho < R$, where $C_+ = \{\xi \in B_R(0) \setminus B_{|R-\rho|}(0) \mid \xi_1 > 0\}$. In the limit $R \to \infty$, the integral of an arbitrary function with compact support over the domain $E_{2,R-\sigma}$ therefore converges for every $\sigma > 0$ to its integral over the set $\tilde{E}_{2,\sigma}$ defined in (2.12); see again Figure 2.

So, we get in the limit $R\to\infty$ for every $\sigma>0$ that

$$\lim_{R\to\infty} RM_\theta(R-\sigma) = \lim_{R\to\infty}\left(\int_{E_{1,R-\sigma}} + 2\int_{E_{2,R-\sigma}}\right)\frac{2\bar p_\theta(\xi)}{\sqrt{|\xi|^2-\sigma^2}}\frac{R}{\sqrt{(2R-\sigma)^2-|\xi|^2}}\,\mathrm{d}\xi$$
$$= \left(\int_{\tilde E_{1,\sigma}} + 2\int_{\tilde E_{2,\sigma}}\right)\frac{\bar p_\theta(\xi)}{\sqrt{|\xi|^2-\sigma^2}}\,\mathrm{d}\xi.$$

Thus, taking the difference of this identity for θ and $-\theta$, we find because of the symmetry $\bar p_{-\theta}(\xi) = \bar p_\theta(-\xi)$ that

$$\lim_{R\to\infty} R\big(M_\theta(R-\sigma) - M_{-\theta}(R-\sigma)\big) = \left(\int_{\tilde E_{1,\sigma}} + 2\int_{\tilde E_{2,\sigma}}\right)\frac{\bar p_\theta(\xi)-\bar p_\theta(-\xi)}{\sqrt{|\xi|^2-\sigma^2}}\,\mathrm{d}\xi.$$

However, since the integrand is odd and the domain $\tilde E_{1,\sigma}$ is point symmetric, meaning that $\tilde E_{1,\sigma} = -\tilde E_{1,\sigma}$, the integration over $\tilde E_{1,\sigma}$ vanishes. ■

Still, this integral equation for the averaged pressure contains contributions from outside the plane E, but at least for small values of σ, that is, close to the axis of the detector, these contributions are restricted to a small area around this plane.

Lemma 2.4. *Let $\tilde M_\theta$ be given by (2.10) for some function $\bar p_\theta \in C^1_{\mathrm{c}}(\mathbb{R}^2)$ with support inside a ball $B_d(0)$ for some $d>0$, and let $\tilde E_{2,\sigma}$ be defined by (2.12).*

Then,

$$\tilde M_\theta(\sigma) = 2\int_\sigma^\infty \frac{\arcsin(\frac{\sigma}{r})}{\sqrt{1-(\frac{\sigma}{r})^2}}\,\tilde p_\theta(r,0)\,\mathrm{d}r + C_\theta(\sigma) \quad \text{for all} \quad \sigma\in(0,d), \tag{2.13}$$

where we set $\tilde p_\theta(\xi) = \bar p_\theta(\xi) - \bar p_\theta(-\xi)$ and $|C_\theta(\sigma)| \le 2\sigma^2\sqrt{2}\|\nabla\tilde p_\theta\|_\infty(\frac{\pi}{2}+\log(\frac{d}{\sigma}))$.

Proof. Parametrizing the domain $\tilde E_{2,\sigma}$ in (2.10) with polar coordinates, we find for $\sigma>0$ that

$$\tilde M_\theta(\sigma) = \int_\sigma^\infty\int_{-\arcsin(\frac{\sigma}{r})}^{\arcsin(\frac{\sigma}{r})} \frac{r\tilde p_\theta(r\cos\varphi, r\sin\varphi)}{\sqrt{r^2-\sigma^2}}\,\mathrm{d}\varphi\,\mathrm{d}r.$$

Now, by the mean value theorem, we have that

$$|\tilde p_\theta(r\cos\varphi,r\sin\varphi) - \tilde p_\theta(r,0)| \le 2r\|\nabla\tilde p_\theta\|_\infty|\sin\tfrac{\varphi}{2}| \le r\sqrt{2}\|\nabla\tilde p_\theta\|_\infty|\sin\varphi|$$

for all $\varphi\in[-\frac{\pi}{2},\frac{\pi}{2}]$. Thus, for $\varphi\in[-\arcsin(\frac{\sigma}{r}),\arcsin(\frac{\sigma}{r})]$, we have

$$|\tilde p_\theta(r\cos\varphi,r\sin\varphi) - \tilde p_\theta(r,0)| \le \sigma\sqrt{2}\|\nabla\tilde p_\theta\|_\infty.$$

Therefore, we find that

$$\tilde M_\theta(\sigma) = 2\int_\sigma^\infty \frac{r\tilde p_\theta(r,0)}{\sqrt{r^2-\sigma^2}}\arcsin(\tfrac{\sigma}{r})\,\mathrm{d}r + C_\theta(\sigma),$$

where the error C_θ can be estimated by

$$\begin{aligned}|C_\theta(\sigma)| &\le 2\sqrt{2}\|\nabla\tilde{p}_\theta\|_\infty \int_\sigma^d \frac{r\sigma}{\sqrt{r^2-\sigma^2}} \arcsin(\tfrac{\sigma}{r})\,\mathrm{d}r \\ &= 2\sigma\sqrt{2}\|\nabla\tilde{p}_\theta\|_\infty \left[\arcsin(\tfrac{\sigma}{r})\sqrt{r^2-\sigma^2}\Big|_\sigma^d + \int_\sigma^d \frac{\sigma}{r}\,\mathrm{d}t\right] \\ &\le 2\sigma^2\sqrt{2}\|\nabla\tilde{p}_\theta\|_\infty(\tfrac{\pi}{2}+\log(\tfrac{d}{\sigma})). \qquad \blacksquare\end{aligned}$$

Ignoring the systematic error term C_θ, the integral equation (2.13) can be explicitly solved for the averaged pressure via a Mellin transform.[4] Explicitly, applying the Mellin transform $\mathcal{M}$ to (2.13), interchanging the order of integration, and substituting σ by $z = \frac{\sigma}{r}$, we get that

$$\begin{aligned}\mathcal{M}(\tilde{M}_\theta - C_\theta)(w) &= \sqrt{\frac{2}{\pi}} \int_0^\infty \int_\sigma^\infty \frac{\arcsin(\frac{\sigma}{r})}{\sqrt{1-(\frac{\sigma}{r})^2}} \sigma^{-\frac{1}{2}+\mathrm{i}w} \tilde{p}_\theta(r,0)\,\mathrm{d}r\,\mathrm{d}\sigma \\ &= \sqrt{\frac{2}{\pi}} \int_0^\infty \int_0^1 \frac{\arcsin(z)}{\sqrt{1-z^2}} z^{-\frac{1}{2}+\mathrm{i}w}\,\mathrm{d}z\, \tilde{p}_\theta(r,0) r^{\frac{1}{2}+\mathrm{i}w}\,\mathrm{d}r.\end{aligned}$$

Therefore, we obtain for the Mellin transform $\mathcal{M}_r\tilde{p}_\theta$ of the function $r \mapsto r\tilde{p}_\theta(r,0)$ the relation

$$\mathcal{M}_r\tilde{p}_\theta(w) = \left[2\int_0^1 \frac{\arcsin(z)}{\sqrt{1-z^2}} z^{-\frac{1}{2}+\mathrm{i}w}\,\mathrm{d}z\right]^{-1} \mathcal{M}(\tilde{M}_\theta - C_\theta)(w)$$

for all $w \in \mathbb{R}$.

However, since we can in general control the systematic error $C_\theta(\sigma)$ only for small values of σ, we cannot estimate the Mellin transform $\mathcal{M}C_\theta$ sufficiently well. We therefore should try to solve the integral equation (2.13) by using only small values of σ.

This problem is similar to the inversion of the interior Radon transform; see [20, 22]. Indeed, by linearizing the arcsine around zero, we find that the integral equation (2.13) becomes

$$\frac{1}{\sigma}\tilde{M}_\theta(\sigma) = 2\int_\sigma^\infty \frac{\tilde{p}_\theta(r,0)}{\sqrt{r^2-\sigma^2}}\,\mathrm{d}r + \tilde{C}_\theta(\sigma)$$

for some error $\tilde{C}_\theta$ which tends to zero for $\sigma \to 0$. The integral on the right-hand side is none other than the Abel transform[5] of the function $r \mapsto \frac{1}{r}\tilde{p}_\theta(r)$, which is the same as the Radon transform of the rotationally invariant function $f : \mathbb{R}^2 \to \mathbb{R}$ with $f(\xi) = \frac{1}{|\xi|}\tilde{p}_\theta(|\xi|, 0)$.

Though the interior Radon transform is not injective and thus not exactly invertible, it is possible to approximatively reconstruct the function $\tilde{p}_\theta(r,0)$ in some interval $r \in [0,\delta]$ using only the measurements $\tilde{M}_\theta(\sigma)$ for $\sigma \in [0, \delta+\tilde{\delta}]$ for some $\tilde{\delta} > 0$, where the error gets smaller when increasing $\tilde{\delta}$; see, for example, [5].

[4] We recall that the Mellin transform $\mathcal{M}f$ of a function $f \in L^2((0,\infty))$ is defined by $\mathcal{M}f(w) = \frac{1}{\sqrt{2\pi}}\int_0^\infty f(z)z^{-\frac{1}{2}+\mathrm{i}w}\,\mathrm{d}z$, $w \in \mathbb{R}$, and can be explicitly inverted via $f(z) = \frac{1}{\sqrt{2\pi}}\int_{-\infty}^\infty \mathcal{M}f(w)z^{-\frac{1}{2}-\mathrm{i}w}\,\mathrm{d}w$, $z \in (0,\infty)$; see, for example, [29, Chapter 9.3] or [30, Chapter 12].

[5] The Abel transform $\mathcal{A}f : (0,\infty) \to (0,\infty)$ of a function $f \in C^1((0,\infty))$ with bounded support is defined by $\mathcal{A}f(\sigma) = 2\int_\sigma^\infty \frac{r}{\sqrt{r^2-\sigma^2}} f(r)\,\mathrm{d}r$, $\sigma > 0$, and its inverse is explicitly given by $f(r) = -\frac{1}{\pi}\int_r^\infty \frac{(\mathcal{A}f)'(\sigma)}{\sqrt{\sigma^2-r^2}}\,\mathrm{d}r$, $r > 0$; see, for example, [30, Chapter 8.10].

From these data, we can then reconstruct from relation (2.6), again with an inversion of the interior Radon transform, the function $p(\xi,0)-p(-\xi,0)$ for sufficiently small values $\xi\in\mathbb{R}^2$. If the object is placed, for instance, in the half-plane $\{x\in\mathbb{R}^3\mid x_1\ge 0\}$, then this gives us explicitly the initial pressure p in the illumination plane $E=\mathbb{R}^2\times\{0\}$ in the vicinity of the origin.

3. Combining focused illumination and focusing detectors. We have seen in section 2 that for a general, sufficiently smooth initial pressure distribution p, we may approximatively reconstruct from the measurements m of the focusing detector this initial pressure in the vicinity of the origin.

To improve the reconstruction, in practice, one attempts to restrict the support of p to the illumination plane E by focusing the laser beam, which generates this initial pressure, to illuminate as much as possible only the plane E; see, for example, [31, 28].

If we thus (without explicitly modelling the illumination) assume that the support of p is contained in a small area

$$E_\delta=\{x\in\mathbb{R}^3\mid x_3\in(-\delta,\delta)\}$$

around the illumination plane E for a sufficiently small $\delta>0$, then the systematic error C_θ in the integral equation (2.13) may be neglected, and we get an inversion formula for p in the illumination plane.

Corollary 3.1. *Let $\tilde M_\theta$ be given by (2.10) for some function $\bar p_\theta\in C^1_{\mathrm{c}}(\mathbb{R}^2)$ with support inside the domain $B_d(0)\cap E_\delta$ for some $d>0$ and $\tilde E_{2,\sigma}$ defined by (2.12).*

Then, we have for $\sigma\ge\delta$ the integral equation

$$\tilde M_\theta(\sigma)=2\int_\sigma^\infty\frac{r}{\sqrt{r^2-\sigma^2}}\arcsin(\tfrac{\delta}{r})\tilde p_\theta(r,0)\,\mathrm{d}r+C_{\theta,\delta}(\sigma), \tag{3.1}$$

where $|C_{\theta,\delta}(\sigma)|\le 2\delta^2\sqrt{2}\|\nabla\tilde p_\theta\|_\infty(\frac{\pi}{2}+\log(\frac{d}{\delta}))$.

Proof. From the definition (2.10) of $\tilde M_\theta$, we have for $\sigma\ge\delta$ that

$$\tilde M_\theta(\sigma)=\int_\sigma^\infty\int_{-\arcsin(\frac{\delta}{r})}^{\arcsin(\frac{\delta}{r})}\frac{r\tilde p_\theta(r\cos\varphi,r\sin\varphi)}{\sqrt{r^2-\sigma^2}}\,\mathrm{d}\varphi\,\mathrm{d}r.$$

As in the proof of Lemma 2.4, we then use for $\varphi\in[-\arcsin(\frac{\delta}{r}),\arcsin(\frac{\delta}{r})]$ the estimate

$$|\tilde p_\theta(r\cos\varphi,r\sin\varphi)-\tilde p_\theta(r,0)|\le r\sqrt{2}\|\nabla\tilde p_\theta\|_\infty|\sin\varphi|\le\delta\sqrt{2}\|\nabla\tilde p_\theta\|_\infty.$$

Therefore, we find that

$$\tilde M_\theta(\sigma)=2\int_\sigma^\infty\frac{r\tilde p_\theta(r,0)}{\sqrt{r^2-\sigma^2}}\arcsin(\tfrac{\delta}{r})\,\mathrm{d}r+C_{\theta,\delta}(\sigma)$$

with the error term $C_{\theta,\delta}$ being bounded by

$$\begin{aligned}|C_{\theta,\delta}(\sigma)|&\le 2\sqrt{2}\|\nabla\tilde p_\theta\|_\infty\int_\sigma^d\frac{r\delta}{\sqrt{r^2-\sigma^2}}\arcsin(\tfrac{\delta}{r})\,\mathrm{d}r\\&=2\delta\sqrt{2}\|\nabla\tilde p_\theta\|_\infty\left[\arcsin(\tfrac{\delta}{r})\sqrt{r^2-\sigma^2}\Big|_\sigma^d+\int_\sigma^d\frac{\sqrt{r^2-\sigma^2}}{\sqrt{r^2-\delta^2}}\frac{\delta}{r}\,\mathrm{d}t\right]\\&\le 2\delta^2\sqrt{2}\|\nabla\tilde p_\theta\|_\infty(\tfrac{\pi}{2}+\log(\tfrac{d}{\delta})).\qquad\blacksquare\end{aligned}$$

Since the integral on the right-hand side of (3.1) is simply the Abel transform of the function $r \mapsto \arcsin(\frac{\delta}{r})\tilde{p}_\theta(r,0)$, we can (up to the uniformly bounded error $C_{\theta,\delta}$) explicitly solve the equation for $\tilde{p}_\theta$. Therefore, (3.1) allows us to reconstruct the values $\tilde{p}_\theta(r,0)$ for all $r \geq \delta$. Then, we may use (2.13) for $\sigma < \delta$ to recover the values $\tilde{p}_\theta(r,0)$ for $r \leq \delta$.

4. Quantitative reconstruction. To reconstruct not only the initial pressure but also the involved physical quantities of the object, in particular the optical absorption coefficient, we not only need to model the elastic wave P in the photoacoustic experiment via (2.1), but we should also model the light propagation in the medium.

Considering only elastic scattering, the propagation of the laser light can be modelled with a Boltzmann transport equation, the so-called radiative transfer equation, for the density of photons $\psi_\vartheta(t,x)$ at the position $x \in \mathbb{R}^3$ at the time $t \in \mathbb{R}$ moving in the direction $\vartheta \in S^2$ of the form

$$\frac{1}{c}\partial_t\psi_\vartheta(t,x) + \langle\vartheta,\nabla_x\psi_\vartheta(t,x)\rangle + \mu_{\mathrm{t}}(x)\psi_\vartheta(t,x) = \frac{\mu_{\mathrm{s}}(x)}{4\pi}\int_{S^2}\Theta(x,\tilde{\vartheta},\vartheta)\psi_{\tilde{\vartheta}}(t,x)\,\mathrm{d}s(\tilde{\vartheta}), \tag{4.1}$$

where the extinction or transport coefficient

$$\mu_{\mathrm{t}}(x) = \mu_{\mathrm{a}}(x) + \mu_{\mathrm{s}}(x)$$

is given as the sum of the absorption coefficient μ_{a} and the scattering coefficient μ_s; see, for example, [35]. Here, c denotes the speed of light, and Θ is the phase function; that is, $\Theta(x,\tilde{\vartheta},\vartheta)$ is the probability density that a photon heading into a direction $\tilde{\vartheta} \in S^2$ is scattered at the position $x \in \mathbb{R}^3$ into the direction $\vartheta \in S^2$.

Since in photoacoustic imaging the excitation happens with a short laser pulse with some fixed frequency ν, and the absorption of the light energy happens much faster than the propagation of the acoustic wave, we are not interested in the light distribution as a function of time, but only in the total energy being absorbed at each point. So, let us switch in a first step to the total energy fluence Φ_ϑ originating from photons moving in the direction $\vartheta \in S^2$ as new variable. We have the relation

$$\Phi_\vartheta(x) = h\nu\int_{-\infty}^{\infty}\psi_\vartheta(t,x)c\,\mathrm{d}t, \quad x \in \mathbb{R}^3,\ \vartheta \in S^2,$$

where h denotes the Planck constant.

The transport equation (4.1) is already well studied; see, for example, [6, 33, 1, 8]. However, for the sectional photoacoustic imaging application we have in mind, the scattering in the object under consideration is typically not very large (since otherwise a focusing of the illumination onto a single slice is hardly possible). We therefore think that in this case the very simple approximation of a single scattering medium can serve as a good first model.

In this approximation, one expands the energy fluence Φ_ϑ from photons moving in the direction $\vartheta \in S^2$ in the scattering coefficient μ_{s} up to first order:

$$\Phi_\vartheta(x) \approx \phi_{0,\vartheta}(x) + \phi_{1,\vartheta}(x),$$

where the zeroth order term $\phi_{0,\vartheta}$ shall be the solution of the so-called ballistic part

$$\langle\vartheta,\nabla_x\phi_{0,\vartheta}(x)\rangle = -\mu_{\mathrm{t}}(x)\phi_{0,\vartheta}(x), \quad x \in \mathbb{R}^3, \tag{4.2}$$

of the transport equation (4.1), and the first order term $\phi_{1,\vartheta}$ shall be the solution of the transport equation (4.1) with Φ_ϑ on the right-hand side being replaced by $\phi_{0,\vartheta}$:

$$\langle\vartheta,\nabla_x\phi_{1,\vartheta}(x)\rangle+\mu_{\mathrm{t}}(x)\phi_{1,\vartheta}(x)=\frac{\mu_s(x)}{4\pi}\int_{S^2}\Theta(x,\tilde\vartheta,\vartheta)\phi_{0,\tilde\vartheta}(x)\,\mathrm{d}s(\tilde\vartheta),\quad x\in\mathbb{R}^3. \tag{4.3}$$

All higher order terms in μ_{s} are neglected. Physically, the function $\phi_{0,\vartheta}$ can be interpreted as the fluence generated by nonscattered light, and $\phi_{1,\vartheta}$ as the fluence generated by light which was scattered once.

To specify boundary conditions for these differential equations, let us assume that no absorption or scattering occurs outside the object. Then, an illumination with a widened laser beam from a laser placed infinitely far away in the direction $(-1,0,0)$, which is initially perfectly focused in the plane $E=\{x\in\mathbb{R}^3\mid x_3=0\}$, leads to the boundary conditions

$$\lim_{y_1\to-\infty}\phi_{0,\vartheta}(y)=\Phi^{(0)}\delta_{e_1}(\vartheta)\delta(y_3),\quad (y_2,y_3)\in\mathbb{R}^2, \tag{4.4}$$

$$\lim_{y_1\to-\infty}\phi_{1,\vartheta}(y)=0,\quad (y_2,y_3)\in\mathbb{R}^2. \tag{4.5}$$

Here, δ_ϑ denotes the δ-distribution on the sphere at the point $\vartheta\in S^2$ defined by

$$\frac{1}{4\pi}\int_{S^2}f(\tilde\vartheta)\delta_\vartheta(\tilde\vartheta)\,\mathrm{d}s(\tilde\vartheta)=f(\vartheta)$$

for all functions $f\in C^\infty(S^2)$.

Let us remark that the initial intensity $\Phi^{(0)}$ in (4.4) may also depend on the position y_2 of the incoming laser beam without seriously affecting any of the forthcoming formulas.

Lemma 4.1. *Let $\phi_{0,\vartheta}$ and $\phi_{1,\vartheta}$ be solutions of (4.2) and (4.3) with the initial conditions (4.4) and (4.5) for some given functions $\mu_{\mathrm{t}},\mu_{\mathrm{s}}\in C_{\mathrm{c}}(\mathbb{R}^3)$ and $\Theta\in C_{\mathrm{c}}(\mathbb{R}^3\times S^2\times S^2)$.*

Then, we have for the total energy fluences

$$\bar\phi_j(x)=\frac{1}{4\pi}\int_{S^2}\phi_{j,\vartheta}(x)\,\mathrm{d}s(\vartheta),\quad j=0,1,$$

the expressions

$$\bar\phi_0(x)=\Phi^{(0)}\delta(x_3)\exp\left(-\int_{-\infty}^{x_1}\mu_{\mathrm{t}}(\lambda,x_2,0)\,\mathrm{d}\lambda\right) \tag{4.6}$$

and

$$\bar\phi_1(x)=\frac{\Phi^{(0)}}{4\pi}\int_{\mathbb{R}^3}\frac{\mu_{\mathrm{s}}(y)\delta(y_3)}{|y-x|^2}\Theta\Big(y,e_1,\tfrac{x-y}{|x-y|}\Big)\exp\left(-\int_{\gamma^{y,x}}\mu_{\mathrm{t}}\,\mathrm{d}s\right)\mathrm{d}y, \tag{4.7}$$

where $\gamma^{y,x}$ is the concatenation of the straight lines $(-\infty,y_1]\to\mathbb{R}^3$, $\lambda\mapsto(\lambda,y_2,y_3)$ and $[0,1]\to\mathbb{R}^3$, $\lambda\mapsto y+\lambda(x-y)$.

In particular, we have for $\operatorname{supp}\mu_{\mathrm{s}}\subset B_d(0)$ that

$$\left|\bar\phi_1(x)\right|\le C\log\big(1+\tfrac{4d^2}{x_3^2}\big)\quad\text{for all}\quad x\in B_d(0) \tag{4.8}$$

for some constant $C > 0$.

Proof. Equation (4.2) can be directly integrated, and we immediately find with the boundary condition (4.4) the formula

$$\phi_{0,\vartheta}(x) = \Phi^{(0)}\delta_{e_1}(\vartheta)\delta(x_3)\exp\left(-\int_{-\infty}^{x_1}\mu_{\mathrm{t}}(\lambda, x_2, 0)\,\mathrm{d}\lambda\right),$$

which we can integrate with respect to ϑ over S^2 to obtain (4.6).

The solution of the linear, inhomogeneous differential equation (4.3) is explicitly given by

$$\phi_{1,\vartheta}(x) = \int_{-\infty}^{x_\vartheta}\tilde{\phi}_{0,\vartheta}(x_\vartheta^\perp + \tau\vartheta)\exp\left(-\int_\tau^{x_\vartheta}\mu_{\mathrm{t}}(x_\vartheta^\perp + \lambda\vartheta)\,\mathrm{d}\lambda\right)\mathrm{d}\tau$$

with

$$\begin{aligned}\tilde{\phi}_{0,\vartheta}(y) &= \frac{\mu_{\mathrm{s}}(y)}{4\pi}\int_{S^2}\Theta(y,\tilde{\vartheta},\vartheta)\phi_{0,\tilde{\vartheta}}(y)\,\mathrm{d}s(\tilde{\vartheta}) \\ &= \Phi^{(0)}\mu_{\mathrm{s}}(y)\Theta(y,e_1,\vartheta)\delta(y_3)\exp\left(-\int_{-\infty}^{y_1}\mu_{\mathrm{t}}(\lambda, y_2, 0)\,\mathrm{d}\lambda\right).\end{aligned}$$

Here, we used the notation $x = x_\vartheta^\perp + x_\vartheta\vartheta$ for the decomposition of a space coordinate $x \in \mathbb{R}^3$ into a vector $x_\vartheta^\perp \in \mathbb{R}^3$ orthogonal to ϑ and the component $x_\vartheta = \langle x, \vartheta\rangle$ in the direction of ϑ.

With this, we obtain for the function $\phi_{1,\vartheta}$ the formula

$$\phi_{1,\vartheta}(x) = \Phi^{(0)}\int_0^\infty \mu_{\mathrm{s}}(x-\lambda\vartheta)\Theta(x-\lambda\vartheta, e_1, \vartheta)\exp\left(-\int_{\gamma^{x-\lambda\vartheta,x}}\mu_{\mathrm{t}}\,\mathrm{d}s\right)\delta(x_3-\lambda\vartheta_3)\,\mathrm{d}\lambda.$$

Now, integrating over $\vartheta \in S^2$ and substituting $y = x - \lambda\vartheta$, we find (4.7).

To analyze the behavior for $x_3 \to 0$, we switch in (4.7) to cylindrical coordinates around the point $x \in B_d(0)$ and then find with $f(y;x) = \Phi^{(0)}\mu_{\mathrm{s}}(y)\Theta(y, e_1, \frac{x-y}{|x-y|})\exp(-\int_{\gamma^{y,x}}\mu_{\mathrm{t}}\,\mathrm{d}s)$ that

$$\bar{\phi}_1(x) = \int_0^{2d}\frac{r}{r^2+x_3^2}\int_0^{2\pi} f(x_1 + r\cos\varphi, x_2 + r\sin\varphi, 0; x)\,\mathrm{d}\varphi\,\mathrm{d}r.$$

Since the inner integral is bounded by $2\pi\Phi^{(0)}\|\mu_{\mathrm{s}}\|_\infty\|\Theta\|_\infty$, we end up with an upper bound of the form (4.8). ■

Now, Lemma 4.1 explicitly describes the forward model for the light propagation in the single scattering approximation. According to, for instance, [7], the photoacoustic effect in the medium generates from the total energy fluence $\bar{\Phi} = \frac{1}{4\pi}\int_{S^2}\Phi_\vartheta\,\mathrm{d}s(\vartheta)$, which in our first order approach is approximately given by

$$\bar{\Phi}(x) \approx \bar{\phi}_0(x) + \bar{\phi}_1(x),$$

the initial pressure

$$p(x) = \Gamma(x)\mu_{\mathrm{a}}(x)\bar{\Phi}(x), \quad x \in \mathbb{R}^3, \tag{4.9}$$

where Γ is the Grüneisen parameter,[6] which describes the thermodynamic properties of the medium.

Proposition 4.2. *Let $\phi_{0,\vartheta}$ and $\phi_{1,\vartheta}$ be solutions of (4.2) and (4.3) with the initial conditions (4.4) and (4.5) for some functions $\mu_{\mathrm{t}}, \mu_{\mathrm{s}} \in C^3_{\mathrm{c}}(\mathbb{R}^3)$ and $\Theta \in C^3_{\mathrm{c}}(\mathbb{R}^3 \times S^2 \times S^2)$, and let p be defined by*

$$p(x) = p_0(x) + p_1(x), \quad p_j(x) = \Gamma(x)\mu_{\mathrm{a}}(x)\bar{\phi}_j(x), \quad j = 0, 1,$$

with $\bar{\phi}_j$ given by (4.7) and the additional parameters $\Gamma, \mu_{\mathrm{a}} \in C^3_{\mathrm{c}}(\mathbb{R}^3)$.

Moreover, let P be the solution of the wave equation (2.1), and let the measurements m be given by (2.2) with $\alpha = \frac{\pi}{2}$.

Then, we have that the function $\tilde{M}$, defined as in (2.11), fulfills the relation

$$\tilde{M}_\theta(\sigma) = \int_\sigma^\infty \frac{\hat{p}_\theta(r) - \hat{p}_\theta(-r)}{\sqrt{r^2 - \sigma^2}}\,\mathrm{d}r + C_\theta(\sigma),$$

where $\hat{p}_\theta$ is the Radon transform

$$\hat{p}_\theta(r) = \int_{-\infty}^\infty \hat{p}(\lambda\theta + r\theta^\perp)\,\mathrm{d}\lambda, \quad r \in \mathbb{R},\ \theta \in S^1,$$

of the zeroth order pressure distribution

$$\hat{p}(\xi) = \Phi^{(0)}\Gamma(\xi, 0)\mu_{\mathrm{a}}(\xi, 0)\exp\left(-\int_{-\infty}^{\xi_1} \mu_{\mathrm{t}}(\lambda, \xi_2, 0)\,\mathrm{d}\lambda\right), \quad \xi \in \mathbb{R}^2, \tag{4.10}$$

in the illumination plane, and where the error term C_θ can be bounded by

$$|C_\theta(\sigma)| \le C\sigma(1 + |\log\sigma|^2)$$

for some constant $C > 0$.

Proof. We know from Proposition 2.3 that

$$\tilde{M}_\theta(\sigma) = \int_{\tilde{E}_{2,\sigma}} \frac{\bar{p}_\theta(\xi) - \bar{p}_\theta(-\xi)}{\sqrt{|\xi|^2 - \sigma^2}}\,\mathrm{d}\xi, \tag{4.11}$$

where $\bar{p}_\theta$, defined by (2.3), can be written as

$$\bar{p}_\theta(\xi) = \int_{-\infty}^\infty p_0(\lambda\theta + \xi_1\theta^\perp, \xi_2)\,\mathrm{d}\lambda + \bar{p}_{1,\theta}(\xi)$$

with the first order correction $\bar{p}_{1,\theta}$ being, according to the estimate (4.8) of Lemma 4.1, bounded by

$$|\bar{p}_{1,\theta}(\xi)| \le C\log(1 + \tfrac{4d^2}{\xi_2^2}), \quad \xi \in B_d(0),$$

[6] We have the relation $\Gamma = \frac{1}{C_{\mathrm{p}}}\alpha c_{\mathrm{s}}^2$, where α denotes the thermal expansion coefficient and C_{p} is the specific heat capacity at constant pressure.

for some constants $C > 0$ and $d > 0$ chosen such that the support of μ_{a} and the support of μ_{s} are both contained in the ball $B_d(0)$. Using now the expression (4.6) for $\bar{\phi}_0$ in p_0, we find that

$$\bar{p}_\theta(\xi) = \int_{-\infty}^{\infty} \hat{p}(\lambda\theta + \xi_1\vartheta)\,\mathrm{d}\lambda\,\delta(\xi_2) + \bar{p}_{1,\theta}(\xi) = \hat{p}_\theta(\xi_1)\delta(\xi_2) + \bar{p}_{1,\theta}(\xi).$$

Moreover, we have with the substitution $z = \frac{r}{d}\sin\varphi$ that

$$\begin{aligned}\int_{\tilde{E}_{2,\sigma}\cap B_d(0)} \frac{\log\left(1+\frac{4d^2}{\xi_2^2}\right)}{\sqrt{|\xi|^2-\sigma^2}}\,\mathrm{d}\xi &= \int_\sigma^d \int_{-\arcsin(\frac{\sigma}{r})}^{\arcsin(\frac{\sigma}{r})} \frac{r\log\left(1+\frac{4d^2}{r^2\sin^2\varphi}\right)}{\sqrt{r^2-\sigma^2}}\,\mathrm{d}\varphi\,\mathrm{d}r \\ &= \int_\sigma^d \frac{2r}{\sqrt{r^2-\sigma^2}} \int_0^{\frac{\sigma}{d}} \frac{\log\left(1+\frac{4}{z^2}\right)}{\sqrt{\frac{r^2}{d^2}-z^2}}\,\mathrm{d}z\,\mathrm{d}r.\end{aligned}$$

Then, changing the order of integration, we obtain that

$$\begin{aligned}\int_{\tilde{E}_{2,\sigma}\cap B_d(0)} \frac{\log\left(1+\frac{4d^2}{\xi_2^2}\right)}{\sqrt{|\xi|^2-\sigma^2}}\,\mathrm{d}\xi &= d\int_0^{\frac{\sigma}{d}} \log\left(1+\tfrac{4}{z^2}\right) \int_{\sigma^2}^{d^2} \frac{1}{\sqrt{\rho-\sigma^2}\sqrt{\rho-d^2z^2}}\,\mathrm{d}\rho\,\mathrm{d}z \\ &= 2d\int_0^{\frac{\sigma}{d}} \log\left(1+\tfrac{4}{z^2}\right) \log\left(\frac{\sqrt{1-\frac{\sigma^2}{d^2}}+\sqrt{1-z^2}}{\sqrt{\frac{\sigma^2}{d^2}-z^2}}\right)\mathrm{d}z.\end{aligned}$$

So, we can estimate the integral by

$$\int_{\tilde{E}_{2,\sigma}\cap B_d(0)} \frac{\log\left(1+\frac{4d^2}{\xi_2^2}\right)}{\sqrt{|\xi|^2-\sigma^2}}\,\mathrm{d}\xi \le C\int_0^{\frac{\sigma}{d}} |\log z|\left|\log\left(\tfrac{\sigma^2}{d^2}-z^2\right)\right|\mathrm{d}z \le \tilde{C}\sigma(1+|\log\sigma|^2)$$

for some constants $C, \tilde{C} > 0$. Thus, the contribution of the first order term $\bar{p}_{1,\theta}$ in (4.11) becomes negligible for small values of σ, and we get

$$\begin{aligned}\tilde{M}_\theta(\sigma) &= \int_{\tilde{E}_{2,\sigma}} \frac{\hat{p}_\theta(\xi_1)+\hat{p}_\theta(-\xi_1)}{\sqrt{|\xi|^2-\sigma^2}}\delta(\xi_2)\,\mathrm{d}\xi + C_\theta(\sigma) \\ &= \int_\sigma^\infty \frac{\hat{p}_\theta(\xi_1)+\hat{p}_\theta(-\xi_1)}{\sqrt{\xi_1^2-\sigma^2}}\,\mathrm{d}\xi_1 + C_\theta(\sigma)\end{aligned}$$

with $|C_\theta(\sigma)| \le C\sigma(1+|\log\sigma|^2)$ for some constant $C > 0$. ■

Thus, we may reconstruct the function $\hat{p}_\theta$ from the measurement m_θ for small values of r by performing an approximative inversion of the interior Radon transform. However, this is not enough to reconstruct the physical parameters Γ, μ_{a}, μ_{s}. To do so, we make two photoacoustic experiments with two different illumination directions.

This means we first do a photoacoustic measurement m^-, where we illuminate the sample from the direction $-e_1$ (as in the derivation above), and then do a second measurement m^+, where we illuminate the sample from the opposite direction e_1. Then, we can recover with

Proposition 4.2 the two different initial pressure densities in the illumination plane: $\hat{p}^-$ and $\hat{p}^+$, respectively.

Since we can obtain the formulas for the illumination from the direction e_1 simply by a reflection of the object, we find from (4.10) that the relations between these initial pressure densities and the physical parameters of the object are given by

$$\hat{p}^-(\xi) = \Phi^{(0)}\Gamma(\xi,0)\mu_{\mathrm{a}}(\xi,0)\exp\left(-\int_{-\infty}^{\xi_1}\mu_{\mathrm{t}}(\lambda,\xi_2,0)\,\mathrm{d}\lambda\right), \tag{4.12}$$

$$\hat{p}^+(\xi) = \Phi^{(0)}\Gamma(\xi,0)\mu_{\mathrm{a}}(\xi,0)\exp\left(-\int_{\xi_1}^{\infty}\mu_{\mathrm{t}}(\lambda,\xi_2,0)\,\mathrm{d}\lambda\right). \tag{4.13}$$

These equations can be directly solved for the functions $\Gamma\mu_{\mathrm{a}}$ and μ_{t}, and we obtain the following result.

Proposition 4.3. *Let $\hat{p}^-$ and $\hat{p}^+$ be given by (4.12) and (4.13) for some constant $\Phi^{(0)} > 0$ and some functions $\Gamma, \mu_{\mathrm{a}} \in C_{\mathrm{c}}^1(\mathbb{R}^3)$ and $\mu_{\mathrm{t}} \in C_{\mathrm{c}}(\mathbb{R}^3)$.*

Then, we have

$$\mu_{\mathrm{t}}(\xi,0) = \frac{1}{2}\partial_{\xi_1}\log\frac{\hat{p}^+(\xi)}{\hat{p}^-(\xi)} \quad \text{if} \quad (\xi,0) \in \operatorname{supp}(\Gamma\mu_{\mathrm{a}}). \tag{4.14}$$

Furthermore, we have

$$\Gamma(\xi,0)\mu_{\mathrm{a}}(\xi,0) = \sqrt{\frac{\hat{p}^+(\xi)\hat{p}^-(\xi)}{\Phi^{(0)}\Phi^{(\infty)}(\xi_2)}}, \tag{4.15}$$

where

$$\Phi^{(\infty)}(\xi_2) = \Phi^{(0)}\exp\left(-\int_{-\infty}^{\infty}\mu_{\mathrm{t}}(\lambda,\xi_2,0)\,\mathrm{d}\lambda\right). \tag{4.16}$$

We want to mention that instead of calculating the function $\Phi^{(\infty)}$ via (4.16), this quantity can be easily measured as the energy fluence of the laser beam after having passed the object.

Since the pressure density $\hat{p}$ depends only on the two combinations $\Gamma\mu_{\mathrm{a}}$ and $\mu_{\mathrm{t}} = \mu_{\mathrm{a}} + \mu_{\mathrm{s}}$ of the physical parameters, it is not possible with such a measurement to reconstruct all three physical parameters Γ, μ_{a}, and μ_{s}, but from knowledge of one of them, the other two can be determined. The exact same situation is also encountered in the classical three-dimensional photoacoustic setup; see, for instance, [4].

Conclusions. We have shown a model for photoacoustic sectional imaging with an integrating acoustic detector with the shape of a half-cylinder serving as focusing detector. Close to the focus axis of the acoustic detector, the measurements are then seen to be essentially given by the Abel transform of the initial pressure so that an approximative inversion of the interior Radon transform may be used to recover the initial pressure close to the focus.

In the particular case of a single scattering approximation for the light propagation, this reconstruction can be made quantitative in the sense that the transport coefficient and the product of the absorption coefficient and the Grüneisen parameter can be reconstructed.

REFERENCES

[1] G. Bal, *Inverse transport theory and applications*, Inverse Problems, 25 (2009), 053001.
[2] G. Bal, *Hybrid inverse problems and internal functionals*, in Inverse Problems and Applications: Inside Out. II, G. Uhlmann, ed., Math. Sci. Res. Inst. Publ. 60, Cambridge University Press, Cambridge, UK, 2013, pp. 325–368.
[3] G. Bal, A. Jollivet, and V. Jugnon, *Inverse transport theory of photoacoustics*, Inverse Problems, 26 (2010), 025011.
[4] G. Bal and K. Ren, *Multi-source quantitative photoacoustic tomography in a diffusive regime*, Inverse Problems, 27 (2011), 075003.
[5] C. A. Berenstein and D. F. Walnut, *Local inversion of the Radon transform in even dimensions using wavelets*, in 75 Years of Radon Transform, S. Gindikin and P. Michor, eds., International Press of Boston, Cambridge, MA, 1994, pp. 45–69.
[6] M. Choulli and P. Stefanov, *An inverse boundary value problem for the stationary transport equation*, Osaka J. Math., 36 (1999), pp. 87–104.
[7] B. T. Cox, J. G. Laufer, and P. C. Beard, *The challenges for quantitative photoacoustic imaging*, in Photons Plus Ultrasound: Imaging and Sensing 2009, Proc. SPIE 7177, SPIE, Bellingham, WA, 2009, 717713.
[8] R. Dautray and J.-L. Lions, *Mathematical Analysis and Numerical Methods for Science and Technology, Volume* 6*, Evolution Problems* II, Springer-Verlag, Berlin, 1993.
[9] P. Elbau, O. Scherzer, and R. Schulze, *Reconstruction formulas for photoacoustic sectional imaging*, Inverse Problems, 28 (2012), 045004.
[10] L. C. Evans, *Partial Differential Equations*, Grad. Stud. Math. 19, American Mathematical Society, Providence, RI, 1998.
[11] D. Finch, M. Haltmeier, and Rakesh, *Inversion of spherical means and the wave equation in even dimensions*, SIAM J. Appl. Math., 68 (2007), pp. 392–412.
[12] D. Finch, S. K. Patch, and Rakesh, *Determining a function from its mean values over a family of spheres*, SIAM J. Math. Anal., 35 (2004), pp. 1213–1240.
[13] S. Gratt, K. Passler, R. Nuster, and G. Paltauf, *Photoacoustic section imaging with an integrating cylindrical detector*, Biomed. Opt. Express, 2 (2011), pp. 2973–2981.
[14] A. Kirsch and O. Scherzer, *Simultaneous reconstructions of absorption density and wave speed with photoacoustic measurements*, SIAM J. Appl. Math., 72 (2012), pp. 1508–1523.
[15] P. Kuchment and L. Kunyansky, *Mathematics of thermoacoustic tomography*, European J. Appl. Math., 19 (2008), pp. 191–224.
[16] L. Kunyansky, *Reconstruction of a function from its spherical (circular) means with the centers lying on the surface of certain polygons and polyhedra*, Inverse Problems, 27 (2011), 025012.
[17] L. A. Kunyansky, *Explicit inversion formulae for the spherical mean Radon transform*, Inverse Problems, 23 (2007), pp. 373–383.
[18] L. A. Kunyansky, *A series solution and a fast algorithm for the inversion of the spherical mean Radon transform*, Inverse Problems, 23 (2007), pp. S11–S20.
[19] C. Li and L. V. Wang, *Photoacoustic tomography and sensing in biomedicine*, Phys. Med. Biol., 54 (2009), pp. R59–R97.
[20] A. K. Louis and A. Rieder, *Incomplete data problems in X-ray computerized tomography*, Numer. Math., 56 (1989), pp. 371–383.
[21] R. Ma, A. Taruttis, V. Ntziachristos, and D. Razansky, *Multispectral optoacoustic tomography (MSOT) scanner for whole-body small animal imaging*, Opt. Express, 17 (2009), pp. 21414–21426.
[22] P. Maass, *The interior Radon transform*, SIAM J. Appl. Math., 52 (1992), pp. 710–724.
[23] A. Mamonov and K. Ren, *Quantitative photoacoustic imaging in radiative transport regime*, Commun. Math. Sci., 12 (2014), pp. 201–234.
[24] F. Natterer, *Photo-acoustic inversion in convex domains*, Inverse Probl. Imaging, 6 (2012), pp. 315–320.
[25] R. Nuster, S. Gratt, K. Passler, D. Meyer, and G. Paltauf, *Photoacoustic section imaging using an elliptical acoustic mirror and optical detection*, J. Biomed. Opt., 17 (2012), 030503.
[26] V. P. Palamodov, *A uniform reconstruction formula in integral geometry*, Inverse Problems, 28 (2012), 065014.

[27] G. Paltauf and R. Nuster, *Artifact removal in photoacoustic section imaging by combining an integrating cylindrical detector with model-based reconstruction*, J. Biomed. Opt., 19 (2014), 026014.
[28] G. Paltauf, R. Nuster, and S. Gratt, *Photoacoustic section imaging with integrating detectors*, in Proceedings of ALT 12, Vol. 1, Bern University of Applied Sciences, Burgdorf, Switzerland, 2012.
[29] A. D. Polyanin and A. V. Manzhirov, *Handbook of Integral Equations*, CRC Press, Boca Raton, FL, 1998.
[30] A. D. Poularikas, ed., *Transforms and Applications Handbook*, 3rd ed., Electrical Engineering Handbook Series, CRC Press, Boca Raton, FL, 2010.
[31] D. Razansky, M. Distel, C. Vinegoni, R. Ma, N. Perrimon, R. W. Köster, and V. Ntziachristos, *Multispectral opto-acoustic tomography of deep-seated fluorescent proteins in vivo*, Nat. Photonics, 3 (2009), pp. 412–417.
[32] D. Razansky, C. Vinegoni, and V. Ntziachristos, *Imaging of mesoscopic-scale organisms using selective-plane optoacoustic tomography*, Phys. Med. Biol., 54 (2009), pp. 2769–2777.
[33] P. Stefanov, *Inverse problems in transport theory*, in Inside Out: Inverse Problems and Applications, G. Uhlmann, ed., Math. Sci. Res. Inst. Publ. 47, Cambridge University Press, Cambridge, UK, 2003, pp. 111–131.
[34] L. V. Wang, *Prospects of photoacoustic tomography*, Med. Phys., 35 (2008), pp. 5758–5767.
[35] L. V. Wang and H. Wu, eds., *Biomedical Optics: Principles and Imaging*, Wiley-Interscience, New York, 2007.
[36] M. Xu and L. V. Wang, *Time-domain reconstruction for thermoacoustic tomography in a spherical geometry*, IEEE Trans. Med. Imag., 21 (2002), pp. 814–822.
[37] M. Xu and L. V. Wang, *Universal back-projection algorithm for photoacoustic computed tomography*, Phys. Rev. E, 71 (2005), 016706.
[38] M. Xu and L. V. Wang, *Photoacoustic imaging in biomedicine*, Rev. Sci. Instrum., 77 (2006), 041101.
[39] Y. Xu, D. Feng, and L. V. Wang, *Exact frequency-domain reconstruction for thermoacoustic tomography*—I: *Planar geometry*, IEEE Trans. Med. Imag., 21 (2002), pp. 823–828.
[40] Y. Xu, M. Xu, and L. V. Wang, *Exact frequency-domain reconstruction for thermoacoustic tomography*—II: *Cylindrical geometry*, IEEE Trans. Med. Imag., 21 (2002), pp. 829–833.